Letter

Design, Conformation, and Crystallography of 2-Naphthyl Phenyl Ethers as Potent Anti-HIV Agents

Won-Gil Lee, Albert H. Chan, Krasimir A. Spasov, Karen S. Anderson, and William L Jorgensen

ACS Med. Chem. Lett., **Just Accepted Manuscript** • DOI: 10.1021/acsmedchemlett.6b00390 • Publication Date (Web): 31 Oct 2016

Design, Conformation, and Crystallography of 2-Naphthyl Phenyl Ethers as Potent Anti-HIV Agents

Won-Gil Lee,† Albert H. Chan,‡ Krasimir A. Spasov, ‡ Karen S. Anderson,‡,* and William L. Jorgensen†,*

†Department of Chemistry, Yale University, New Haven, Connecticut 06520-8107, ‡Department of Pharmacology, Yale University School of Medicine, New Haven, CT 06520-8066

.

KEYWORDS: Anti-HIV agents, NNRTIs, protein crystallography.

ABSTRACT: Catechol diethers that incorporate a 7-cyano-2-naphthyl substituent are reported as non-nucleoside inhibitors of HIV-1 reverse transcriptase (NNRTIs). Many of the compounds have 1 – 10 nM potencies towards wild-type HIV-1. An interesting conformational effect allows two unique conformers for the naphthyl group in complexes with HIV-RT. X-ray crystal structures for **4a** and **4f** illustrate the alternatives.

Though significant advances have been made in the treatment of HIV/AIDS, the rate of new infections has remained constant near 2.5 million people per year, the number of people living with the disease continues to increase and now totals about 40 million, and the number of associated deaths in 2015 was 1.2 million.[1] Thus, there remains a pressing need for new therapeutic agents, especially in view of the uncertainties with mutation of the virus and long-term use of the current approved drugs.[2] To this end, we have directed efforts towards the discovery of improved non-nucleoside inhibitors of HIV-1 reverse transcriptase (NNRTIs),[3] which have been a central component of anti-HIV chemotherapy.[4,5] There are five FDA-approved compounds in the class including efavirenz and rilpivirine, which have particular importance since they are components of the one-a-day oral therapies Atripla and Complera, respectively.[4]

Though we have discovered new NNRTIs featuring several different chemotypes, the most promising NNRTIs are in the catechol diether class, which evolved from a docking hit.[6-9] The design **1** led to some extraordinarily potent NNRTIs including the dichloro (R_5, Y = Cl) and difluoro analogues, which have EC_{50} values of 0.055 and 0.320 nM in an assay using human MT-2 cells infected with wild-type (WT) HIV-1.[6] However, the cyanovinyl group in **1** may be viewed as a potential liability in view of its possible participation in Michael additions leading to off-target covalent modifications. Though rilpivirine also has a cyanovinyl group, another NNRTI, fosdevirine, was abandoned after phase IIb clinical trials.[10] Metabolites that arose from cysteine addition of glutathione to its cyanovinyl group were implicated as the source of seizures in 5 of 20 patients.

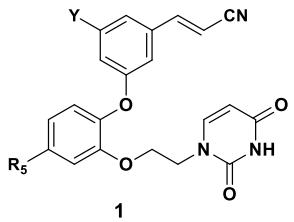

1

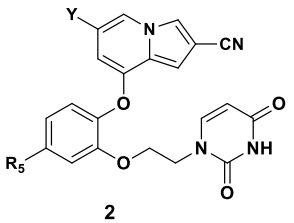

2

In order to avoid the cyanovinyl group, results of free-energy perturbation calculations led us to explore several bicyclic replacements including the indolizine variant **2**, which provided very potent compounds.[5] In particular, the parent **2a** (R_5, Y = H) is impressive. In the standard MT-2 assay it has an EC_{50} of 0.38 nM towards WT HIV-1, while in single-round infectivity assays with $CD4^+$ T cells from blood donors it gives EC_{50} values of 1, 2, and 3 nM towards WT HIV-1, and the most common clinical variants bearing the Y181C and K103N mutations in RT.[9] For comparison, the results for efavirenz are 15, 41, and 806 nM, and for rilpivirine, 13, 51, and 13 nM, respectively.[9] **2a** also remains highly potent towards the K101P variant (1 nM), while efavirenz and rilpivirine are not effective (870 and 1142 nM). In addition, **2a** shows no cytotoxicity towards T cells (CC_{50} > 100 μM), and it has good aqueous solubility, 38 μg/mL. Rilpivirine is significantly more cytotoxic (CC_{50} = 8 μM), and far less soluble (ca. 0.1 μg/mL). However, oddly, in our MT-2 assays with virus containing the single Y181C mutation, **2a** has an EC_{50} of 310 nM, though it remains potent towards the normally more challenging double K103N/Y181C mutant at 11 nM.[5] In the absence of an explanation for the difference in results for Y181C, we have explored additional bicyclic possibilities including 1-naphthyl analogues **3**.[8] Though it was initially unclear if their larger size would be accommodated in the NNRTI binding site, compounds were obtained that performed very well in the MT-2 assays such as **3b** (R_5 = H, Y = F) with EC_{50}s of 1, 8, and 6 nM towards the WT, Y181C, and K103N/Y181C forms.

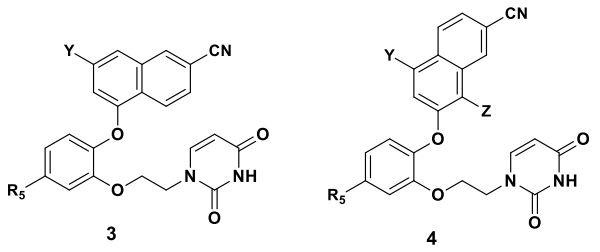

We have also reported numerous x-ray crystal structures for catechol diethers bound to WT HIV-RT and variants.[7-9,11-13] Consistent with the high potencies, the complexes are tightly packed with multiple protein-ligand aryl-aryl interactions and hydrogen bonds. The point is illustrated in Figure 1, which has been rendered from the crystal structure of **3a** (R_5 = Y = H) with WT RT. In particular, the 1-naphthyl group is in well-packed aryl-aryl interactions with Tyr181, Tyr188, and Trp229. In viewing this structure, it is difficult to imagine that the alternative attachment for the naphthyl substituent at the 2-position would not lead to a serious steric clash with Trp229. Nevertheless, structure building with the BOMB program followed by energy minimizations with MCPRO using OPLS force fields was carried out for 2-naphthyl alternatives.[14] Surprisingly, the resultant structures appeared to be viable as long as the cyano group was moved to the 7-position as in **4**. In addition, three possible conformers were suggested by BOMB for the parent **4a** with the cyano group pointed towards Pro95, above Tyr181, and below Trp229 (Figure 2). Thus, motivation arose to pursue the 2-naphthyl series **4**.

As summarized in Scheme 1 and detailed in the Supporting Information, synthesis of the 26 analogues of **4** listed in Table 1 proceeded in a manner similar to that for **3**,[8] though much effort was needed for the preparation of the various 2-hydroxy-7-cyanonaphthalenes. The substituted 2-hydroxynaphthalenes underwent Cu(I)-catalyzed

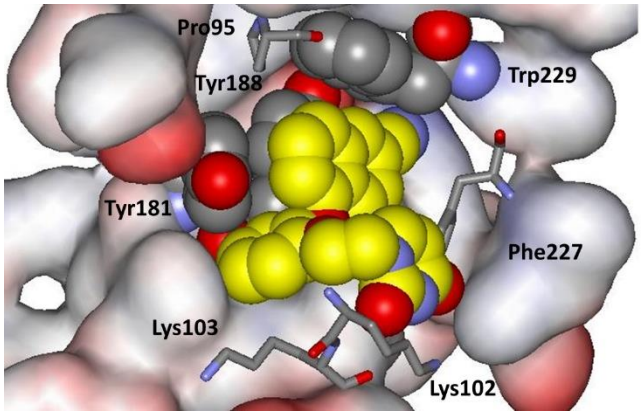

Figure 1. Mixed rendering from the crystal structure of **3a** with wild type HIV-1 reverse transcriptase. Carbon atoms of **3a** are colored yellow. Some residues in front of the ligand have been removed for clarity. The PDB code is 4WE1.

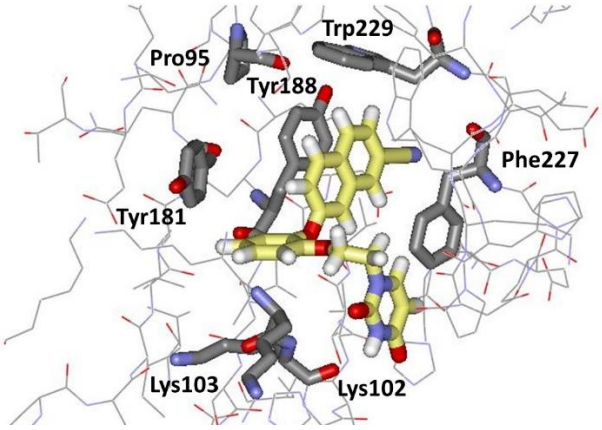

Figure 2. Rendering of a computed structure for the third conformer of **4a** with wild type HIV-1 RT. Carbon atoms of **4a** are colored yellow.

Scheme 1. Synthesis of 2-Naphthyl Phenyl Ethers **4**

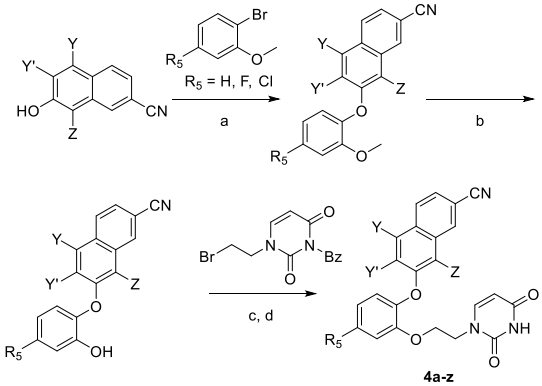

Reagents: (a) CuI, Cs_2CO_3, 2,2,6,6-tetramethyl-3,5-heptanedione, dioxane, 100 °C, 48 h; (b) BBr_3, DCM, -78 °C → 0 °C, 3 h; (c) K_2CO_3, DMF, 60 °C, 3h; (d) NH_4OH, DCM, 16 h.

addition to 2-bromoanisoles to yield 2-naphthyl phenyl ethers. The methoxy group was unmasked with BBr_3 to yield phenols, which were alkylated with *N*-Bz-protected 1-bromoethyluracil. The identity of assayed compounds was confirmed by ^1H and ^{13}C NMR and high-resolution mass spectrometry; HPLC analyses established purity as >95%. Aqueous solubilities were measured using a standard shake-flask procedure, as previously described.[8,15] The procedures for the human MT-2 T-cell assays have also been described in detail.[6-8,16,17] Triplicate assays using the IIIB and variant strains of HIV-1 were performed yielding EC_{50} values as the dose required to achieve 50% protection of the infected MT-2 cells as well as CC_{50} values for inhibition of MT-2 cell growth by 50%.

The activity results for the 2-naphthyl ethers are summarized in Table 1 along with corresponding data for key compounds in the **1** - **3** series and for four FDA-approved NNRTIs. The parent **4a** did turn out to be a good inhibitor of the WT virus with an EC_{50} of 22 nM, though it shows only 2 – 4 μM potency towards the two variant strains. The performance of the isomeric **3a** is substantially better. However, optimization of the substituents in **4** could be expected to provide gains. For R_5, the viable options were

Table 1. Inhibitory Activity (EC_{50}, nM)[a] for HIV-1 and Cytotoxicity (CC_{50}, μM) in MT-2 Cell Assays

	R_5	Z	Y	WT	Y181C	K103N/ Y181C	CC_{50}
1a	F	-	F	0.32	16	85	45
1b	H	-	Cl	0.31	46	24	18
2a	H	-	H	0.38	310	11	>100
2b	F	-	F	0.40	250	10	50
3a	H	-	H	0.53	19	15	>100
3b	H	-	F	1.1	8.0	6.0	>100
3c	F	-	F	1.9	5.6	21	>100
4a	H	H	H	22	2600	4000	15
4b	H	H	Cl	14	890	890	12
4c	H	H	Me	4.9	800	2900	6
4d	H	Cl	F	5.0	90	310	>100
4e	H	Me	F	7.8	60	890	>100
4f	H	Me	Cl	6.2	58	280	>100
4g	H	Cl	Me	5.0	42	120	>100
4h	H	Me	Me	3.5	62	150	>100
4i	H	Me	Et	6.0	150	300	12
4j	H	Me	Pr	21	630	990	15
4k	H	Me	*i*Pr	16	400	100	9
4l	H	Me	*c*PrCH$_2$	18	900	1200	13
4m	H	Me	MeO	17	670	1600	>100
4n	H	Me	EtO	10	200	800	>100
4o	H	Me	MOM	15	690	790	16
4p	H	Me	3-Me	160	NA	1700	5
4q	H	Me	3,4-Me	580	NA	790	>100
4r	F	H	H	26	1200	9400	>100
4s	F	H	Cl	24	1100	4100	>100
4t	F	Cl	F	7.0	72	1600	28
4u	F	Me	F	3.0	31	980	>100
4v	F	F	Me	58	1200	3800	45
4w	F	Me	Cl	3.6	27	500	82
4x	F	Me	Me	1.9	28	410	>100
4y	Cl	Me	F	18	330	NA	6
4z	H	H	6-CN[c]	1300	NA	5600	9
nev[d]				110	NA	NA	>100
efv[d]				2	10	30	15
etv[d]				1	8	5	11
rpv[d]				0.67	0.65	2	8

[a] For 50% protection in MT-2 cells; NA for EC_{50} > CC_{50} or > 100 μM. [b] For 50% inhibition of MT-2 cell growth. [c] 6-CN rather than 7-CN analogue. [d] nevirapine (nev); efavirenz (efv); etravirine (etv); rilpivirine (rpv)

known to be limited[8] such that R_5 = F yields similar potencies as R_5 = H, e.g., **4a** and **4r**, and R_5 = Cl is already too large (**4y** vs. **4u**). Overall, the SAR data are consistent with the structure in Figure 2. For example, a substituent, even CH_3, at C3 of the naphthyl group as in **4p** and **4q** is disfavored since the substituent would be placed over the central phenyl ring. For 2-methyldiphenyl ether such a conformation is not an energy minimum with the OPLS-AA force field; the only two minima are **I** and **II** in which a phenyl hydrogen atom is over a ring center. Furthermore, shift of the cyano group to C6 leads to a 60-fold reduction in WT potency (**4a** vs. **4z**) owing to the expected steric conflict with Trp229.

The structure in Figure 2 and modeling of derivatives did indicate that there should be a wider range of options for Z and especially Y. Z points into the center of the NNRTI

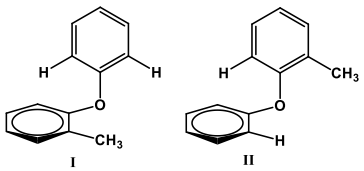

binding site where there is limited space, though Z = Cl and CH_3 could be accommodated with the latter generally preferred as in **4f** and **4g**, and **4t** and **4u**. For Y, a range of options was explored in **4h** – **4o** with Z = CH_3. There was optimism that larger groups for Y would benefit the activity towards the variant viral strains as the group might occupy some of the space vacated by the Y181C mutation. Though this strategy had worked for another NNRTI series,[18] CH_3 emerged as the best choice for Y, and the larger options in **4j** – **4o** showed a narrow range of WT activities, 6 – 21 nM, and poorer performance for the variant HIV strains. It appears that the substituent Y is directed more towards Pro95 and is not optimally oriented to fill the Y181C void.

The analyses above are also consistent with x-ray crystal structures that were obtained for **4a** and **4f** with WT RT (Figure 3). The procedures were similar to those in previous reports[7-9,11-14] and are detailed in the Supporting Information.[19] Strikingly, **4a** is in the conformation with the cyano group projecting over Tyr181. This conformation is only possible when Z = H to avoid a steric clash between

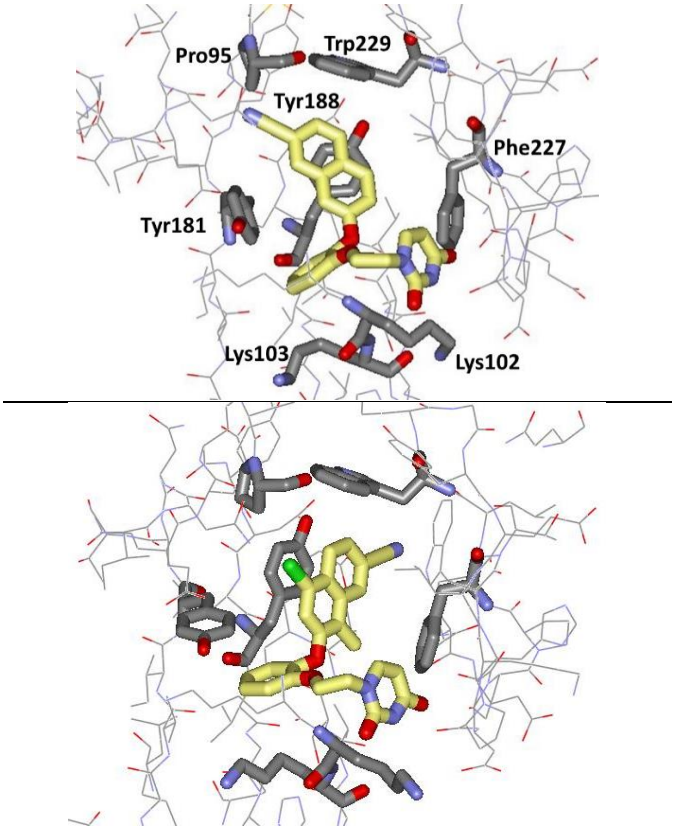

Figure 3. Renderings from the crystal structures of **4a** (top) and **4f** (bottom) with wild type HIV-1 reverse transcriptase.

Table 2. Experimental Aqueous Solubility at pH 6.5 (S in μg/mL) and Computed ClogP

Cmpd	S	ClogP	Cmpd	S	ClogP
1a	10.8	3.09	**4e**	28.2	3.95
1b	510	3.38	**4f**	20.6	4.52
2a	37.9	2.70	nev	167[a]	2.65
2b	43.8	3.14	efv	68.0	4.67
3a	4.3	3.30	etv	<<1[a]	5.22
3b	9.1	3.59	rpv	0.02[a,b]	5.75
3c	82.9	3.73	rpv	0.24[a,c]	5.75

[a] See Ref. 8. [b] pH 7. [c] pH 7.4.

Z and the central phenyl ring, e.g., **4a**, **4b**, **4c**, **4r**, and **4s**. In these cases, the EC_{50} values for the two variant HIV strains are relatively high, which likely arises from loss of the greater contact between the inhibitors and Tyr181 in this conformation. When the 1-position is substituted, the conformation with the cyano group projecting below Trp229 (Figure 2) is expected to be preferred as found for **4f** in Figure 3. Overall, the parent and fluoro-substituted 1-naphthyl analogues **3a** – **3c** have significantly greater potency than the 2-naphthyl compounds **4a** and **4r**. In viewing the crystal structures and computed ones, a simple explanation is not obvious. However, when one optimizes the complexes with the OPLS/CM1A force field[14] for **3a** as in Figure 1 and **4a** as in Figure 2, the protein-ligand interaction energy is lower for **3a** than **4a** by 2.6 kcal/mol. This arises mostly from improved interactions for **3a** with Tyr181, Tyr188, and Trp229 by 0.3, 0.3, and 1.2 kcal/mol, respectively. The preference carries over to the mutant strains, and substitutions at R_5, Y, and Z in **4** were not able to compensate in full.

Overall, **4d - 4i** are the most promising NNRTIs in the 2-naphthyl series. **4g** and **4h** have activities of 5.0 and 3.5 nM towards WT HIV-1, ca. 50 nM towards the Y181C strain, and 120-150 nM toward the double mutant. They also exhibit no T-cell cytotoxicity, CC_{50} > 100 μM. In addition, aqueous solubilities were measured for **4e** and **4f** and fall in the acceptable range for oral drugs (Table 2).[20] The cytotoxicities and solubilities of the approved NNRTIs etravirine and rilpivirine are much less favorable. Previously unreported solubility results for **3b** and **3c** are also provided in Table 2 and with **3a** show the seemingly unconventional pattern of increasing solubility with increasing fluorination. However, similar boosts have been found previously for other cases with fluorine separated from an oxygen atom by 3 carbons.[21,22]

ASSOCIATED CONTENT

Supporting Information. Synthetic procedures, NMR and HRMS spectral data for compounds **4a-z**, and crystallographic details. The crystal structure data for the complexes of **4a** and **4f** with HIV-RT have been deposited in the RCSB Protein Data Bank with the PDB codes 5TEP and 5TER. This information is available free of charge via the Internet at http://pubs.acs.org .

AUTHOR INFORMATION

Corresponding Authors

* karen.anderson@yale.edu

* william.jorgensen@yale.edu

Notes

The authors declare no competing financial interests.

ACKNOWLEDGMENT

Gratitude is expressed to the National Institutes of Health (AI44616, GM32136, GM49551) for research support and for a fellowship for AHC (AI122864). Crystal screening was conducted with support in the Yale Macromolecular X-ray Core Facility (1S10OD018007-01). This work is based upon research conducted at the Northeastern Collaborative Access Team beamlines, which are funded by the National Institute of General Medical Sciences from the National Institutes of Health (P41 GM103403). This research used resources of the Advanced Photon Source, a U.S. Department of Energy (DOE) Office of Science User Facility operated for the DOE Office of Science by Argonne National Laboratory under Contract No. DE-AC02-06CH11357.

ABBREVIATIONS

HIV, human immunodeficiency virus; HIV-RT, HIV reverse transcriptase; NNRTI, non-nucleoside inhibitor of HIV-RT; Bz, benzoyl; DCM, dichloromethane; DMF, dimethylformamide; HPLC, high-performance liquid chromatography.

REFERENCES

(1) Wang, H. *et al.* Estimates of global, regional, and national incidence, prevalence, and mortality of HIV, 1985-2015: the Global Burden of Disease Study 2015. *Lancet HIV* **2016**, *3*, e361-e387.

(2) Reynolds, C.; de Koning, C. B.; Pelly, S. C.; van Otterlo, W. A. L.; Bode, M. L. In search of a treatment for HIV – current therapies and the role of non-nucleoside reverse transcriptase inhibitors (NNRTIs). *Chem. Soc. Rev*. **2012**, *41*, 4657-4670.

(3) Jorgensen, W. L. Computer-aided discovery of anti-HIV agents. *Bioorg. Med. Chem*. **2016**, *24*, 4768-4778.

(4) De Clercq, E. The Nucleoside Reverse Transcriptase Inhibitors, Nonnucleoside Reverse Transcriptase Inhibitors, and Protease Inhibitors in the Treatment of HIV Infections (AIDS). *Adv. Pharmacol.* **2013**, *67*, 317-358.

(5) Zhan, P.; Chen, X.; Li, D.; Fang, Z.; De Clercq, E.; Liu, X. HIV-1 NNRTIs: Structural Diversity, Pharmacophore Similarity, and Implications for Drug Design. *Med. Res. Rev*. **2013**, *33*, E1-E72.

(6) Bollini, M.; Domaoal, R. A.; Thakur, V. V.; Gallardo-Macias, R.; Spasov, K. A.; Anderson, K. S.; Jorgensen, W. L. Computationally-Guided Optimization of a Docking Hit to Yield Catechol Diethers as Potent Ani-HIV Agents. *J. Med. Chem.* **2011**, *54*, 8582-8591.

(7) Lee, W.-G.; Gallardo-Macias, R.; Frey, K. M.; Spasov, K. A.; Bollini, M.; Anderson, K. S.; Jorgensen, W. L. Picomolar Inhibitors of HIV Reverse Transcriptase Featuring Bicyclic Replacement of a Cyanovinylphenyl Group. *J. Am. Chem. Soc.* **2013**, *135*, 16705-16713.

(8) Lee, W.-G.; Gallardo-Macias, R.; Frey, K. M.; Spasov, K. A.; Bollini, M.; Anderson, K. S.; Jorgensen, W. L. Picomolar Inhibitors of HIV Reverse Transcriptase: Design and Crystallography of Naphthyl Phenyl Ethers. *ACS Med. Chem. Lett.* **2014**, *5*, 1259-1262.

(9) Gray, W. T.; Frey, K. M.; Laskey, S. B.; Mislak, A. C.; Spasov, K. A.; Lee, W.-G.; Bollini, M.; Siliciano, R. F.; Jorgensen, W. L.; Anderson, K. S. Potent Inhibitors Active against HIV Reverse Transcriptase with K101P, a Mutation Conferring Rilpivirine Resistance. *ACS Med. Chem. Lett.* **2015**, *6*, 1075-1079.

(10) Castellino, S.; Groseclose, M. R.; Sigafoos, J.; Wagner, D.; de Serres, M.; Polli, J. W.; Romach, E.; Myer, J.; Hamilton, B. Central Nervous System Disposition and Metabolism of Fosdevirine (GSK2248761), a Non-Nucleoside Reverse Transcriptase Inhibi-

tor: An LC-MS and Matrix-Assisted Desorption/Ionization Imaging MS Investigation into Central Nervous System Toxicity. *Chem. Res. Toxicol*. **2013**, *26*, 241-251.

(11) Frey, K. M.; Bollini, M.; Mislak, A. C.; Cisneros, J. A.; Gallardo-Macias, R.; Jorgensen, W. L.; Anderson, K. S. Crystal Structures of HIV-1 Reverse Transcriptase with Picomolar Inhibitors Reveal Key Interactions for Drug Design. *J. Am. Chem. Soc.* **2012**, *134*, 19501-19503.

(12) Frey, K. M.; Gray, W. T.; Spasov, K. A.; Bollini, M.; Gallardo-Macias, R.; Jorgensen, W. L.; Anderson, K. S. Structure-Based Evaluation of C5 Derivatives in the Catechol Diether Series Targeting HIV-I Reverse Transcriptase. *Chem. Biol. Drug Des*. **2014**, *83*, 541-549.

(13) Frey, K. M.; Puleo, D. E.; Spasov, K. A.; Bollinin, M.; Jorgensen, W. L.; Anderson, K. S. Structure-Baed Evaluation of Non-nucleoside Inhibitors with Improved Potency and Solubility That Target HIV Reverse Transcriptase Variants. *J. Med. Chem.* **2015**, *58*, 2737-2745.

(14) Jorgensen, W. L. Efficient Drug Lead Discovery and Optimization. *Acc. Chem. Res*. **2009**, *42*, 724-733.

(15) Baka, E.; Comer, J. E. A; Takács-Novák, K. Study of equilibrium solubility measurement by saturation shake-flask method using hydrochlorothiaide as model compound. *J. Pharm. Biomed. Anal*. **2008**, *46*, 335-341.

(16) Lin, T. S.; Luo, M. Z.; Liu, M. C.; Pai, S. B.; Dutschman,G. E.; Cheng, Y. C. Antiviral activity of 2',3'-dideoxy-β-L-5-fluorocytidine (β-L-EddC) and 2',3'-dideoxy-β-L-cytidine (β-L-ddC) against hepatitis B virus and human immunodeficiency virus type 1 in vitro. *Biochem. Pharmacol.* **1994**, *47*, 171-174.

(17) Ray, A. S.; Yang, Z.; Chu, C. K.; Anderson, K. S. Novel use of a guanosine prodrug approach to convert 2',3'-didehydro-2',3'-dideoxyguanosine into a viable antiviral agent. *Antimicrob. Agents Chemother.* **2002**, *46*, 887-891.

(18) Bollini, M.; Gallardo-Macias, R.; Spasov, K. A.; Tirado-Rives, J.; Anderson, K. S.; Jorgensen, W. L. Optimization of benzyloxazoles as non-nucleoside inhibitors of HIV-1 reverse transcriptase to enhace Y181C potency. *Bioorg. Med. Chem. Lett*. **2013**, *23*, 1110-1133.

(19) The resolution limits for the structures are 3.10 and 2.70 Å, and they have been deposited with PDB IDs of 5TEP and 5TER, respectively.

(20) Jorgensen, W. L.; Duffy, E. M. Prediction of drug solubility from structure. *Adv. Drug Deliv. Rev*. **2002**, *54*, 355-366.

(21) Böhm, H.-J.; Banner, D.; Bendels, S.; Kansy, M.; Kuhn, B.; Müller, K.; Obst-Sander, U.; Stahl, M. Fluorine in Medicinal Chemsitry. *ChemBioChem* **2004**, *5*, 637-643.

(22) Walker, M. A. Improving Solubility by Structural Modification. *Top. Med. Chem*. **2015**, *9*, 69-106.